Published OnlineFirst March 29, 2012; DOI: 10.1158/0008-5472.CAN-11-3185

Therapeutics, Targets, and Chemical Biology

Cancer Research

Coxsackievirus B3 Is an Oncolytic Virus with Immunostimulatory Properties That Is Active against Lung Adenocarcinoma

Shohei Miyamoto[1], Hiroyuki Inoue[1,2], Takafumi Nakamura[3], Meiko Yamada[4], Chika Sakamoto[1], Yasuo Urata[4], Toshihiko Okazaki[1], Tomotoshi Marumoto[1], Atsushi Takahashi[1], Koichi Takayama[2], Yoichi Nakanishi[2], Hiroyuki Shimizu[5], and Kenzaburo Tani[1]

Abstract

Although oncolytic virotherapy is a promising anticancer therapy, antitumor efficacy is hampered by low tumor selectivity. To identify a potent and selective oncolytic virotherapy, we carried out large-scale two-step screening of 28 enteroviral strains and found that coxsackievirus B3 (CVB3) possessed specific oncolytic activity against nine human non–small cell lung cancer (NSCLC) cell lines. CVB3-mediated cytotoxicity was positively correlated with the expression of the viral receptors, coxsackievirus and adenovirus receptor, and decay-accelerating factor, on NSCLC cells. *In vitro* assays revealed that the CVB3 induced apoptosis and phosphoinositide 3-kinase/Akt and mitogen-activated protein (MAP)/extracellular signal-regulated (ERK) kinase (MEK) survival signaling pathways, leading to cytotoxicity and regulation of CVB3 replication. Intratumoral injections of CVB3 elicited remarkable regression of preestablished NSCLC tumors *in vivo*. Furthermore, administrations of CVB3 into xenografts on the right flank resulted in significantly durable regression of uninjected xenografts on the left flank, where replication-competent CVB3 was detected. All treatments with CVB3 were well tolerated without treatment-related deaths. In addition, after CVB3 infection, NSCLC cells expressed abundant cell surface calreticulin and secreted ATP as well as translocated extranuclear high-mobility group box 1, which are required for immunogenic cell death. Moreover, intratumoral CVB3 administration markedly recruited natural killer cells and granulocytes, both of which contributed to the antitumor effects as shown by depletion assays, macrophages, and mature dendritic cells into tumor tissues. Together, our findings suggest that CVB3 is a potent and well-tolerated oncolytic agent with immunostimulatory properties active against both localized and metastatic NSCLC. *Cancer Res; 72(10); 2609–21. ©2012 AACR.*

Introduction

Oncolytic viruses are self-replicating, tumor-selective viruses, with an ability to directly induce cancer cell death, and have emerged as a promising treatment platform for cancer therapy (1).

Over the past 2 decades, clinical trials of oncolytic virotherapies using a range of DNA and RNA viruses including coxsackievirus A21 (CVA21), measles virus, Newcastle disease virus, and reovirus have been reported or are underway (2–5). Clinical development of these therapies has progressed to late phase trials. However, the antitumor efficacy of oncolytic viruses has yet to attain the potential anticipated in preclinical studies.

RNA viruses seem to be a safer modality, as most single-stranded RNA viruses replicate in the host cytosol without a DNA phase. Therefore, they lack the genotoxicity caused by integration of the viral genome into the host DNA. In particular, enteroviruses, members of the *Picornaviridae* family, a diverse group of small RNA viruses have emerged as promising candidates for cancer treatment (6–9). Their use has several therapeutic advantages: these viruses immediately induce robust cytolytic changes during cell-to-cell infection, they do not possess oncogenes that may lead to tumorigenesis, and they can be easily genetically manipulated by reverse genetics systems for the rescue of positive-strand RNA viruses from complementary DNA (10, 11). Furthermore, most nonpolio enteroviruses are common and highly prevalent and are mainly associated with asymptomatic infection or mild disease (12). Although CVA21 is reportedly a potent oncolytic enterovirus against

Authors' Affiliations: [1]Division of Molecular and Clinical Genetics, Medical Institute of Bioregulation; [2]Research Institute for Diseases of the Chest, Graduate School of Medical Sciences, Kyushu University, Fukuoka; [3]Core Facility for Therapeutic Vectors, The Institute of Medical Science, The University of Tokyo; [4]Oncolys BioPharma Inc.; and [5]Department of Virology II, National Institute of Infectious Diseases, Tokyo, Japan

Note: Supplementary data for this article are available at Cancer Research Online (http://cancerres.aacrjournals.org/).

S. Miyamoto and H. Inoue contributed equally to this work.

Corresponding Author: Kenzaburo Tani, Division of Molecular and Clinical Genetics, Medical Institute of Bioregulation, Kyushu University, 3-1-1 Maidashi, Higashi-ku, Fukuoka 812-8582, Japan. Phone: 81-92-642-6449; Fax: 81-92-642-6444; E-mail: taniken@bioreg.kyushu-u.ac.jp

doi: 10.1158/0008-5472.CAN-11-3185

©2012 American Association for Cancer Research.

Downloaded from cancerres.aacrjournals.org on April 19, 2015. © 2012 American Association for Cancer Research.

Published OnlineFirst March 29, 2012; DOI: 10.1158/0008-5472.CAN-11-3185

miscellaneous human cancer cells (8, 9, 13), CVA21-treated mice died of lethal myositis with paralysis (14).

Apart from direct oncolysis, another important component of the sustained therapeutic advantage of oncolytic viruses depends on their ability to trigger antitumor immune responses (15). Robust viral replication in tumors provides immunologic damage-associated molecular pattern (DAMP) signals, augmenting the immunogenicity of the tumor microenvironment (16). Previous studies showed that several oncolytic viruses could induce adaptive antitumor immunity by tumor-specific CTL responses (17). However, little is known about how preceding innate immunity shapes the antitumor effects and whether oncolytic viruses cause immunogenic cancer cell death by similar mechanisms to chemotherapeutic agents, such as calreticulin (CRT) exposure, ATP release, or high-mobility group box 1 (HMGB1) translocation (18).

The focus of this study was to identify a novel oncolytic virus from screening 28 different strains of human enteroviruses, which had high tolerability when administered in mouse xenograft models, and to clarify the viral cytocidal mechanism by scrutinizing the apoptotic and antitumor immunogenic potential of the virus.

Materials and Methods

Mice

Female BALB/c nude mice were purchased from Charles River Japan. All animal experiments were carried out under the Guidelines for Animal Experiments of Kyushu University and Law 105 Notification 6 of the Japanese Government.

Cell lines

The non–small cell lung cancer (NSCLC; A549, H1299, and H460), colon cancer (Caco-2), pancreatic cancer (AsPC-1), renal cancer (A-498 and Caki-1), rhabdomyosarcoma (RD), T-cell leukemia (HuT 102), bone marrow stromal (HS-5), and normal lung fibroblast (MRC-5) cell lines were purchased from the American Type Culture Collection. NSCLC cell lines (PC-9, EBC-1, and LK-2) were obtained from the Health Science Research Resources Bank in Japan. Human lung squamous cell carcinoma cell lines (QG-56 and QG-95) were provided by Dr Y. Ichinose (National Kyushu Cancer Center; ref. 19). The other NSCLC cell lines (LK-87 and Sq-1) were obtained from Cell Resource Center for Biomedical Research, Tohoku University. Human cell lines of colon cancer (DLD-1), pancreatic cancer (PANC-1), breast cancer (MCF7), cervical cancer (HeLa S3), and normal lung fibroblast (NHLF) were provided by Dr T. Fujiwara (Okayama University). No authentication besides PCR tests that showed free from *Mycoplasma* contamination was done for all of cell lines used.

Production of enteroviruses

The 28 strains of enteroviruses tested were obtained from H. Shimizu (National Institute of Infectious Diseases, Japan) and were propagated in HeLa and RD cells. The $TCID_{50}$/mL on these cell monolayers was determined as previously described (20).

Crystal violet staining

Viable cells at 72-hour postinfection with enteroviruses at appropriate multiplicity of infection (MOI) for 1 hour were assessed by crystal violet staining as previously described (21). Cell survival rates were calculated by Multi Gauge software version 3.2 (FUJIFILM).

Flow cytometry analysis

Cells were incubated with a monoclonal antibody against coxsackievirus and adenovirus receptor (CAR; Upstate) followed by incubation with fluorescein isothiocyanate (FITC)-conjugated anti-mouse immunoglobulin G, or phycoerythrin (PE)-conjugated antibody decay-accelerating factor (DAF; BD Biosciences). For analysis of surface CRT, NSCLC cells infected with Coxsackievirus B3 (CVB3; MOI = 10) was analyzed by flow cytometric analysis (22). Data were obtained with a FACSCalibur (BD Biosciences) and analyzed by FlowJo software Version 7.6 (Tree Star Inc.).

MTS assay for cell viability

In vitro cell viability experiments using cells infected with CVB3 were carried out by a Cell Titer 96 AQueous Non-Radioactive Cell Proliferation Assay (Promega) following the manufacturer's instructions.

In vitro inhibition assays

Cells were pretreated with serum-free media containing the specific phosphoinositide 3-kinase (PI3K) inhibitor LY294002 (Santa Cruz Biotechnology), the PTEN inhibitor bisperoxovanadium (bpV, HOpic; Merck), or the mitogen-activated protein (MAP)/extracellular signal-regulated kinase (ERK; MEK) inhibitor PD0325901 (Wako) for 1 hour, and then infected with CVB3 (MOI = 10) for 1 hour. For apoptosis inhibition assay, A549 cells were pretreated with the pan-caspase inhibitor, z-VAD-fmk (100 or 200 μmol/L for 1 hour; R&D Systems), exposed to CVB3 at MOI of 0.01 or 0.1 for 1 hour, and replaced in indicated concentrations of z-VAD-fmk for additional 48 hours.

siRNA transfection assay

siRNAs specific for human CAR and a negative control were designed and synthesized by BONAC in Japan. Transfection of A549 cells with siRNAs was carried out with Lipofectamine 2000 (Invitrogen) according to the manufacturer's protocol. Following 72-hour incubation after transfection, cells were infected with CVB3 at MOI of 0.01 for MTS assays.

Western blot analysis

Cell lysate samples were resolved by SDS-PAGE and immunoblotted (21). The primary antibodies used were monoclonal antibodies against PARP (Biovision), phospho-Akt (Ser473; BioLegend), and β-actin (Santa Cruz Biotechnology). Densitometry analysis was conducted with LAS3000 (FUJIFILM) and Multi Gauge software version 3.2.

Annexin V staining and cell-cycle analysis

Apoptotic cells after CVB3 infection were determined with the Annexin V–PE apoptosis detection kit (BD Biosciences) according to the manufacturer's instructions. For cell-cycle

Downloaded from cancerres.aacrjournals.org on April 19, 2015. © 2012 American Association for Cancer Research.

Published OnlineFirst March 29, 2012; DOI: 10.1158/0008-5472.CAN-11-3185

analysis, the cells were fixed in 70% ethanol, incubated with RNase A (50 μg/mL), stained with 10 μg/mL propidium iodide (PI), and analyzed with a FACS-Calibur.

ATP release assay

After cell death induction, secreted extracellular ATP was measured with the luciferin-based ENLITEN ATP Assay (Promega) according to the manufacturer's protocol.

Immunofluorescence microscopy

Cells fixed with 4% paraformaldehyde were permeabilized with 0.3% Triton X-100 for 10 minutes, incubated with anti-HMGB1 antibody for 30 minutes followed by incubation with Alexa Fluor 488–conjugated secondary antibody (Molecular Probes), and analyzed by a fluorescence microscope BZ-9000 (KEYENCE).

In vivo therapeutic studies

A549 cells (5×10^6 cells) or EBC-1 cells (3×10^6 cells) were injected subcutaneously into the right or bilateral flanks of nude mice. When tumors reached diameters of 0.4 to 0.6 cm, the tumors on the right flank were inoculated with CVB3 (5×10^6 $TCID_{50}$) once on day 2 or with the same doses of CVB3 on days 2, 4, 6, 8, and 10.

The RB6-8C5 rat hybridoma cell line producing the anti-mouse Gr-1 monoclonal antibody was provided by Dr T. Yokomizo (Kyushu University). For granulocyte depletion, nude mice implanted with 5×10^6 A549 cells were intraperitoneally injected with 300 μg rat anti–Gr-1 antibody (99.7% elimination of circulating polymorphonuclear neutrophils). For natural killer (NK) cell depletion, nude mice were intraperitoneally injected with rabbit polyclonal anti-asialo GM1 antibody (Wako; ref. 23). The tumor volume was calculated as length × width × width/2 and expressed as means ± SEM. Animals were euthanized when the tumor diameter exceeded 1.0 cm.

Tumor-infiltrating lymphocytes

The excised tumors were gently homogenized with sharp syringes, incubated for 90 minutes in RPMI-1640 containing collagenase (Invitrogen). For innate immunity subpopulations, the cells were stained with anti-mouse DX-5-FITC, Gr-1-PE, F4/80-APC, or CD11c-APC antibodies for 30 minutes. For mature dendritic cells (DC), the cells were stained with anti-mouse CD86-FITC, CD80-PE, CCR7-PerCP, and CD11c-APC antibody for 30 minutes. For cytolytic effector cells, the cells were stained with anti-mouse DX-5-FITC, Gr-1-PerCP, and CD107a-PE antibody for 30 minutes (24) and analyzed by a FACS Calibur.

Statistical analyses

Statistical analyses were conducted with GraphPad Prism 5.0d software package (GraphPad Software Inc.). Statistical analysis was conducted using a 2-tailed unpaired Student *t* test, one-way ANOVA followed by Tukey multiple comparison test, or nonparametric Mann–Whitney *U* test. $P < 0.05$ was considered statistically significant. Survival curves were plotted according to the Kaplan–Meier method (log-rank test).

Results

Sequential two-step screening identifies CVB3 as a candidate for oncolytic virus against NSCLC

To identify a safer and more potent oncolytic enterovirus, we carried out a large-scale screening of 28 strains of enteroviruses for oncolytic activity. This screening was carried out *in vitro* against 12 different human cancer cell lines and the HS-5 normal bone marrow stromal cell line using crystal violet staining. Several enteroviruses displayed marked cytotoxic effects (Fig. 1A) in a dose-dependent manner (Supplementary Fig. S1A and S1B). The Coxsackievirus B group, CVB2 (Ohio-1), CVB3 (Nancy), and CVB4 (J.V.B.) were of particular interest, as they showed exclusive oncolytic effects on the A549 and LK-87 NSCLC cell lines (Fig. 1A). In a secondary screen, we evaluated the oncolytic efficacy of CVB2, CVB3, and CVB4 against 9 additional NSCLC cell lines and 2 normal lung cell lines. Unexpectedly, only CVB3 infection induced marked cytolysis in 100% (9 of 9) NSCLC cell lines of diverse histologic subtypes, that is, adenocarcinoma (A549), squamous cell carcinoma (EBC-1), and large cell carcinoma (H460) even at an MOI of 0.001. However, CVB3 did not induce cytolysis against normal lung fibroblast cell lines even at an MOI as high as 10 (Fig. 1B). Accordingly, we employed CVB3 harboring potent and specific cytolytic activity as a candidate virus for oncolytic virotherapy against NSCLC.

Correlation of CVB3-mediated cytotoxicity and expression levels of surface receptors on NSCLC Cells

We next compared the expression level of the CVB3 receptors, CAR and DAF (25) on various human NSCLC and normal lung cell lines. NSCLC cell lines expressed moderate to high levels of CAR, whereas normal lung cell lines expressed very low levels of CAR. The expression of DAF was similarly high in the NSCLC and normal lung cell lines (Fig. 2A). The oncolytic activity of CVB3 significantly correlated with a number that was equal to the percentage of CAR-expressing cells multiplied by the percentage of DAF-expressing cells ($r = -0.92$, $P < 0.0001$), whereas 2 normal lung cell lines were unaffected (Fig. 2B). The results of the *in vitro* MTS cell viability assays confirmed this correlation in a time-dependent manner (Fig. 2C). To thereby elucidate the role of CAR in the cytolytic effects of CVB3, CVB3-infected A549 cells were analyzed in the presence of siRNA-mediated functional CAR knockdown. Flow cytometric analyses confirmed the reduction of CAR expression by 92% in A549 cells transfected with CAR-specific siRNA (Supplementary Fig. S2). The inhibition of CAR significantly abrogated the cytotoxicity of CVB3 ($P < 0.001$; Fig. 2D).

Contribution of caspase-mediated apoptosis and PI3K/Akt or MEK/ERK signaling pathways to CVB3-mediated cytotoxicity in NSCLC cells

To determine whether CVB3 induced apoptosis in NSCLC cells treated with CVB3 (MOI = 0.1), we examined the cleavage of PARP by caspases, an execution marker of apoptosis. Western blot analysis revealed cleaved PARP (85 kDa) in CVB3-treated A549 and LK-2 NSCLC cells, but not in CVB3-

Downloaded from cancerres.aacrjournals.org on April 19, 2015. © 2012 American Association for Cancer Research.

Published OnlineFirst March 29, 2012; DOI: 10.1158/0008-5472.CAN-11-3185

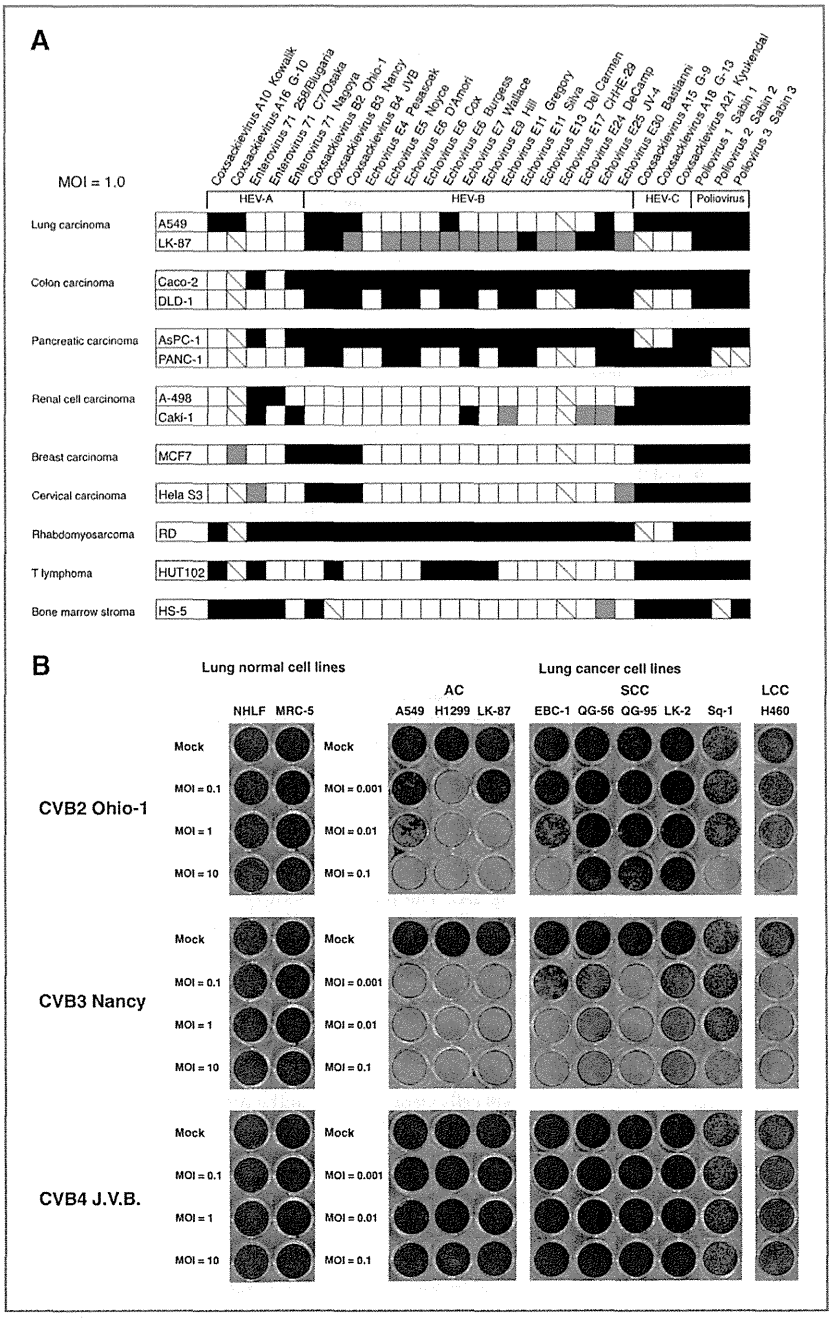

Figure 1. Sequential 2-step screenings to identify a potent *oncolytic virus candidate*. A, various cancer cell lines and HS-5 cells were infected with 28 strains of enterovirus at an MOI of 1.0 and incubated for 1 hour. At 72 hours postinfection, cell viability was assessed by crystal violet staining. Black, gray, white, and hashed boxes indicate greater than 50% cytotoxicity, less than 50% cytotoxicity, no cytotoxicity, and not analyzed, respectively. HEV-A, human enterovirus A; HEV-B, human enterovirus B; HEV-C, human enterovirus C. B, various human NSCLC and normal lung cell lines were infected with CVB2, CVB3, and CVB4 for 72 hours at MOIs of 0.001, 0.01, and 0.1 for NSCLC cell lines and MOIs of 0.1, 1.0, and 10 for normal cell lines, respectively. Cell viability was assessed by crystal violet staining. AC, adenocarcinoma; SCC, squamous cell carcinoma; LCC, large cell carcinoma.

treated MRC-5 normal lung cells (Fig. 3A). We analyzed externalization of phosphatidylserine and DNA fragmentation, hallmarks of apoptosis. CVB3-treated A549 cells showed a greater proportion of apoptotic (AnnexinV$^+$/7-AAD$^-$) and necrotic (AnnexinV$^+$/7-AAD$^+$) cells than LK-2 cells, correlating with CAR expression (Fig. 3B). Similarly, exposure of A549 cells to CVB3 induced more sub-G_1 cells with DNA fragmentation than LK-2 cells, correlating with CAR expression. In contrast, neither Annexin V positivity nor DNA fragmentation was induced in CVB3-treated MRC-5 cells (Fig. 3C). To determine whether

Downloaded from cancerres.aacrjournals.org on April 19, 2015. © 2012 American Association for Cancer Research.

Published OnlineFirst March 29, 2012; DOI: 10.1158/0008-5472.CAN-11-3185

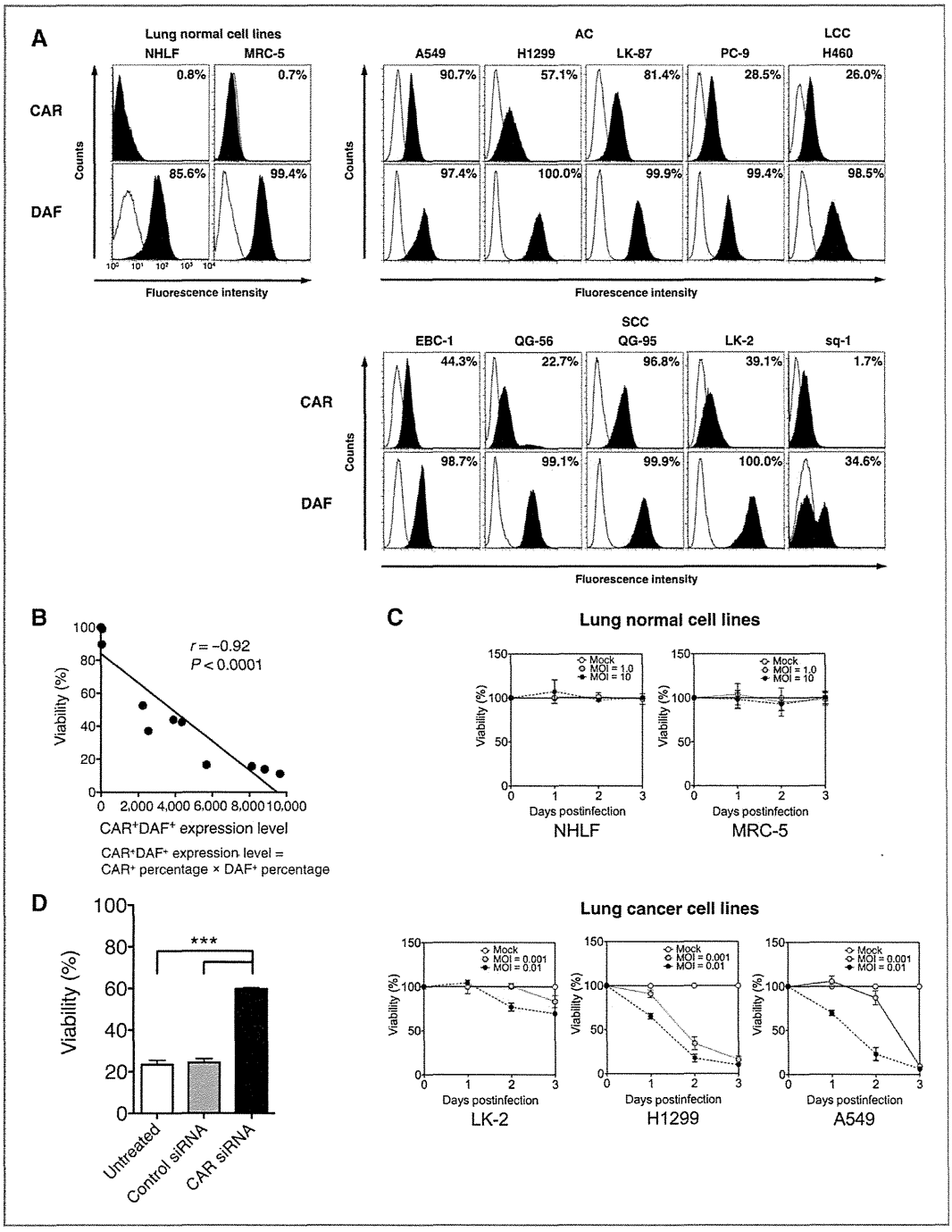

Figure 2. Expression profile of surface CAR and DAF on normal lung and NSCLC cells and its correlation with CVB3-mediated cytotoxicity. A, surface expression of CVB3 receptors on various lung cell lines was quantified by flow cytometry. Histograms represent the measured fluorescence of cells incubated with an isotype control antibody (unshaded) and anti-CAR or anti-DAF antibody (shaded). B, correlation between expression of CAR and DAF and cell viability at 72 hours after CVB3 infection ($r = -0.92$; $P < 0.0001$). C, cells infected with CVB3 at indicated MOIs was analyzed at indicated time points for cell viability by MTS assay. Each value was normalized to Opti-MEM–treated cells (mock) and represents the mean ± SD. D, A549 cells transfected with CAR-specific siRNA or control siRNA were infected with CVB3 (MOI = 10), and assessed by MTS cell viability assay at 48 hours after CVB3 infection. Each value was normalized to mock and represents the mean ± SD. ***, $P < 0.001$.

Downloaded from cancerres.aacrjournals.org on April 19, 2015. © 2012 American Association for Cancer Research.

Published OnlineFirst March 29, 2012; DOI: 10.1158/0008-5472.CAN-11-3185

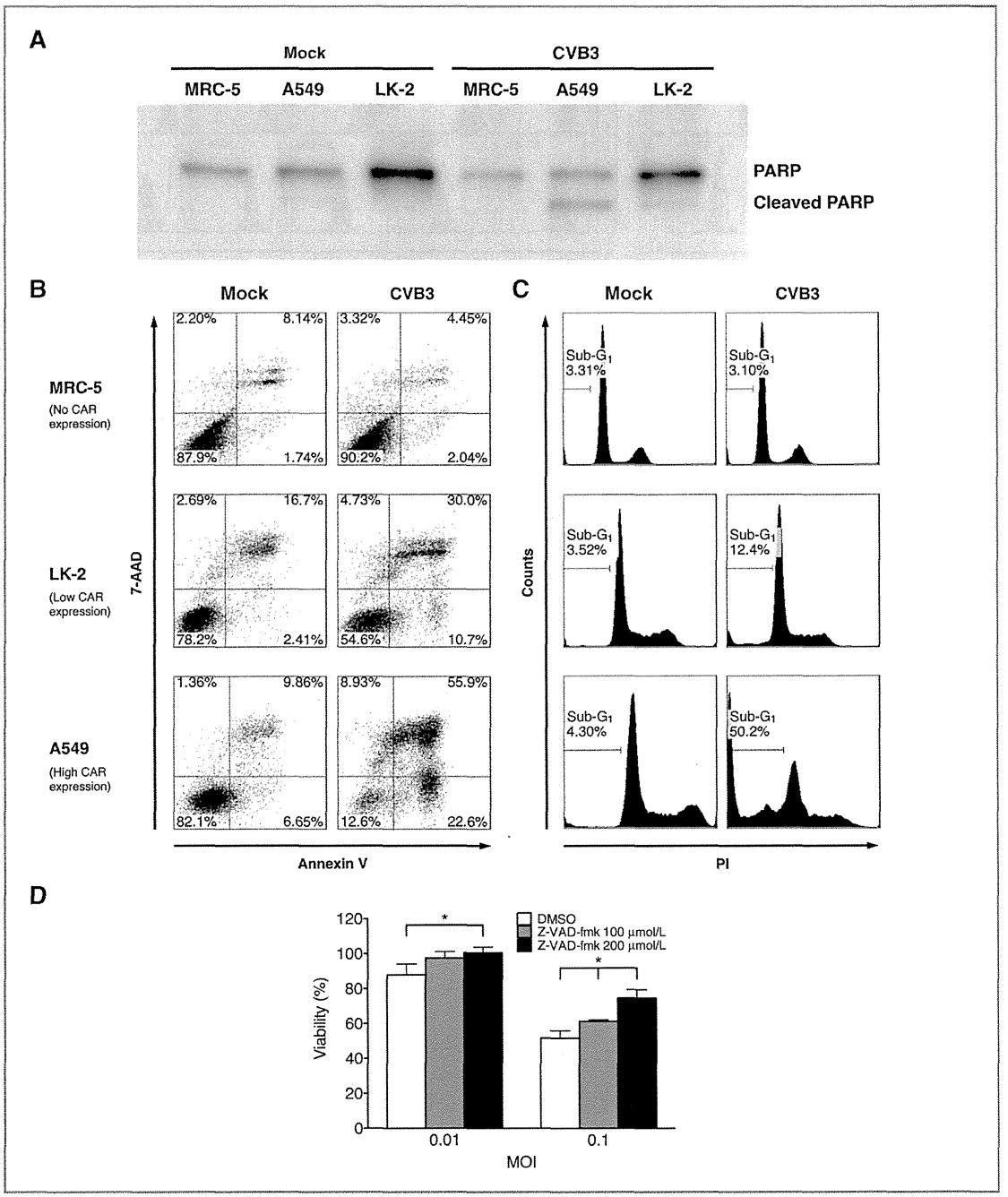

Figure 3. Correlation between caspase-dependent apoptosis and CVB3-mediated cytotoxicity in NSCLC cells. Lung cell lines infected with CVB3 (MOI = 0.1) were analyzed 24 hours later. A, each cellular lysate obtained was subjected to immunoblot analysis. Full-length PARP (116 kDa) and cleaved PARP (85 kDa) are shown. B, early apoptotic population was represented as Annexin V–PE^+/7-AAD^- cells. C, each histogram PI depicts the population of cells in G_1 and G_2–M, and the apoptotic subdiploid peak (sub-G_1). D, cells pretreated with dimethyl sulfoxide (DMSO) or z-VAD-fmk and incubated with mock or CVB3 at indicated MOIs were subjected to MTS cell viability assays. *, $P < 0.05$.

Downloaded from cancerres.aacrjournals.org on April 19, 2015. © 2012 American Association for Cancer Research.

Published OnlineFirst March 29, 2012; DOI: 10.1158/0008-5472.CAN-11-3185

CVB3-inducible apoptosis contributed to CVB3-mediated cytotoxicity against A549 cells, we treated them with the pan-caspase inhibitor, z-VAD-fmk. CVB3-mediated cytotoxicity was slightly but significantly reduced when z-VAD-fmk was added in a dose-dependent manner (Fig. 3D).

Because PI3K/Akt signaling pathways mediate CVB3 replication in human cancer cells (26), we investigated whether CVB3 infection could activate Akt phosphorylation (p-Akt) in A549 cells. CVB3 infection induced substantial p-Akt expression on the Ser-473 residue, peaking at 15 minutes postinfection (Fig. 4A and B), prompting us to examine the effects of pretreatment with LY294002, a specific PI3K inhibitor, or bpV, an inhibitor of PTEN that antagonizes PI3K activity, on p-Akt expression levels in CVB3-treated A549 cells. LY294002 reduced but bpV enhanced the level of p-Akt induced by CVB3 infection (Fig. 4C and D). In addition, LY294002 significantly diminished but bpV significantly augmented CVB3-mediated cytotoxicity against A549 cells at 14 hours after infection in a dose-dependent manner, whereas no cytotoxicity was observed when either of these agents were used in the absence of CVB3 (Fig. 4E and F). To unravel the relationship between p-Akt expression and CVB3 replication, we examined the effects of LY294002 or bpV on release of CVB3 progeny from CVB3-treated A549 cells. The CVB3 titer was significantly reduced when LY294002 was added, whereas it was increased almost 2-fold when bpV was added ($P < 0.05$; Fig. 4G), showing that PI3K/Akt pathway was involved in CVB3 replication. Furthermore, addition of a potent MEK inhibitor PD0325901, which blocks

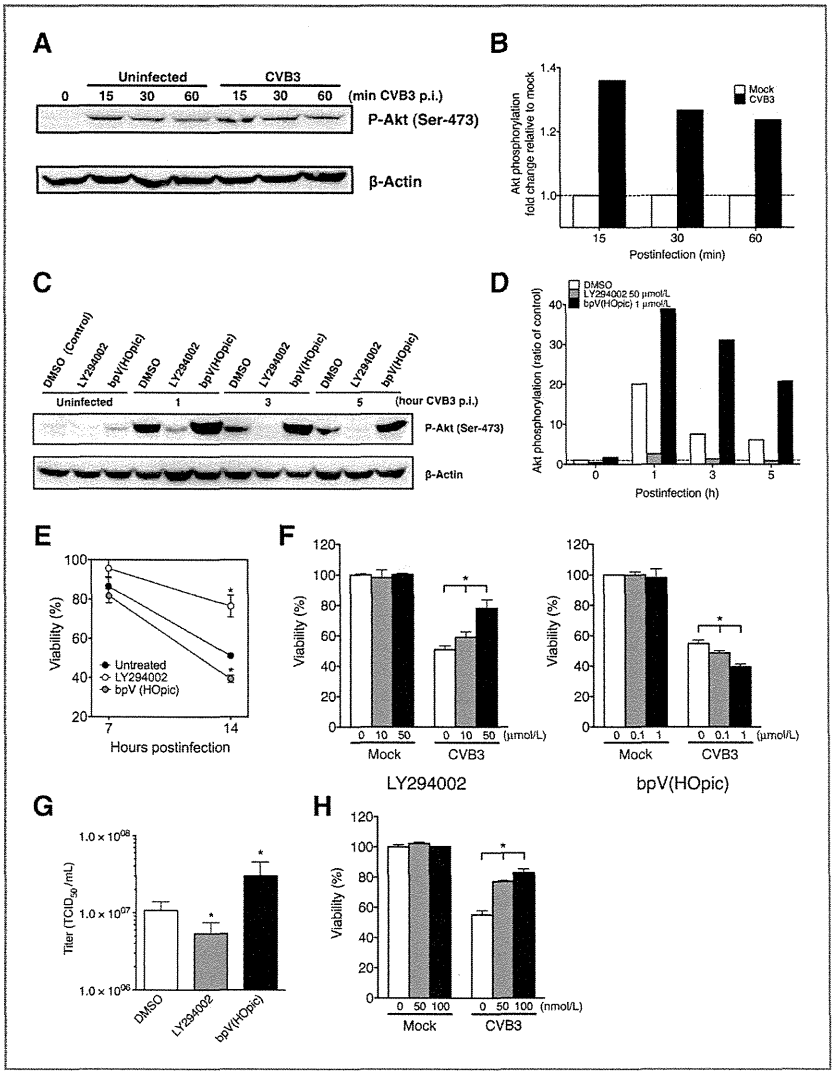

Figure 4. Correlation between 2 survival signaling pathways and CVB3-mediated cytotoxicity and viral replication in human NSCLC cell lines. A549 cells infected with CVB3 (MOI = 0.1) were analyzed. A and B, each cell lysate collected at indicated time points was subjected to Western blotting assay for p-Akt on Ser-473 detection. Results normalized to mock were evaluated by densitometric analysis using Multi Gauge. C and D, p-Akt expression in A549 cells treated with LY294002 or bpV followed by CVB3 infection was determined by Western blotting analysis. E, A549 cells were treated with 50 μmol/L LY294002, 1 μmol/L bpV, or DMSO for 1 hour, infected with CVB3 or Opti-MEM for 1 hour, incubated for 7 or 14 hours, and subjected to MTS cell viability assays. *, $P < 0.05$. F, A549 cells treated as above were incubated for 14 hours at various concentrations of LY294002 or bpV and subjected to MTS cell viability assays. *, $P < 0.05$. G, supernatants from the LY294002- or bpV-treated A549 cells after 14 hours of CVB3 infection were collected and viral titer was determined. *, $P < 0.05$. H, A549 cells were treated with various concentrations of MEK inhibitor PD0325901 or DMSO for 1 hour, followed by CVB3 infection, incubated for 14 hours, and subjected to MTS cell viability assay. *, $P < 0.05$.

Downloaded from cancerres.aacrjournals.org on April 19, 2015. © 2012 American Association for Cancer Research.

Published OnlineFirst March 29, 2012; DOI: 10.1158/0008-5472.CAN-11-3185

phosphorylation of ERK, to CVB3 infection significantly decreased cytotoxicity against A549 cells in a dose-dependent manner, whereas PD0325901 alone did not have any effect (Fig. 4H).

Efficacy studies in nude mice

We next evaluated *in vivo* oncolytic effects of CVB3 and its tolerability in nude mice bearing subcutaneous NSCLC xenografts. A single dose of intratumoral CVB3 administered into A549 xenografts significantly suppressed tumor growth ($P < 0.01$; Fig. 5A). In addition, the survival rate was significantly improved in CVB3-treated mice compared with untreated mice ($P = 0.0008$; Fig. 5B). To evaluate tolerability and dose-dependent oncolytic effects, 5 consecutive doses of CVB3 were intratumorally administered into A549 xenografts. The treatment with CVB3 elicited significant tumor regression in a dose-dependent manner ($P < 0.05$; Fig. 5C), with significantly prolonged survival ($P = 0.0004$). Moreover, half of the CVB3-treated mice achieved complete regression of the tumor (Fig. 5D). Similarly, in the EBC-1 human squamous cell carcinoma xenograft model, intratumoral 5 administrations of CVB3 revealed significant antitumor effects. All CVB3-treated mice achieved complete tumor elimination with a significantly prolonged survival rate (Fig. 5E and F). For H1299 human adenocarcinoma xenograft, similar potent antitumor effects with complete tumor rejection were observed in all of CVB3-treated mice (Supplementary Fig. S3). Notably, none of the mice died of side effects during these treatments.

To further investigate systemic oncolytic effects of CVB3, we used a mouse model with bilaterally preestablished subcutaneous A549 xenografts. Five consecutive CVB3 administrations into the right flank tumors only significantly suppressed the growth of both the CVB3-injected tumor and the distant untreated tumor when compared with untreated mice ($P < 0.05$; Fig. 5G), and displayed a significantly prolonged survival rate ($P = 0.0021$) and no lethality (Fig. 5H). To clarify the mechanism by which CVB3 exerted antitumor effects against the contralateral tumor, we investigated whether the supernatants derived from disrupted untreated tumors or from CVB3-treated tumors had oncolytic activity against A549 cells. The supernatants derived from both CVB3-treated and CVB3-untreated tumors destroyed A549 cells (Fig. 5I), showing that replication-competent CVB3 did exist in untreated contralateral tumors.

Immunologic assays

As preapoptotic exposure to CRT and ATP release and postapoptotic HMGB1 are required for immunogenic cell death induced by chemotherapeutic agents such as anthracyclines and oxaliplatins (18), we examined whether CVB3 infection promoted similar effects on NSCLC cells. CVB3 treatment induced abundant surface exposure of CRT (Fig. 6A) on both A549 and H1299 cells, and active secretion of extracellular ATP was in dose- and time-dependent manner (Fig. 6B). In addition, CVB3 infection resulted in substantial release of HMGB1, another determinant of immunogenicity, from the nuclei of both A549 and H1299 cells into the cytosol (Fig. 6C).

We next evaluated the effects of intratumoral CVB3 administration on tumor-infiltrating immune cells in A549-bearing mice. CVB3 administration recruited significantly greater accumulation of NK cells, granulocytes, macrophages, and DCs into the tumor bed compared with the controls ($P < 0.01$; Fig. 7A and B). The tumor-infiltrating DCs expressed significantly higher levels of the costimulatory molecules CD80, CD86, and the maturation marker CCR7 in CVB3-treated mice compared with untreated mice ($P < 0.05$; Fig. 7C). It has been reported that mobilized CD107a expression, a cytolytic degranulation marker, correlates with NK cell–mediated lytic potential (27), and that granulocytes contribute to the antitumor effect of the oncolytic measles virus (28). We therefore explored the effects of CVB3 treatment on tumor-infiltrating CD107a-harbouring NK cells and granulocytes. A higher density of NK cells as well as granulocytes mobilized CD107a to their cell surface in CVB3-treated mice compared with untreated mice (Fig. 7D). We further investigated the role of endogenous NK cells or granulocytes on the CVB3-mediated antitumor effect by depleting tumor-bearing mice of NK cells or granulocytes. Depletion of either NK cells or granulocytes significantly abrogated the therapeutic effect of CVB3 ($P < 0.05$; Fig. 7E), illustrating their substantial contribution to CVB3-induced antitumor responses.

Discussion

Lung cancer is the world's leading cause of cancer death, resulting in more than 1 million deaths per year worldwide (29). However, standard conventional therapies have produced limited cures, highlighting the need to develop novel therapeutic modalities (30). Here, we successfully identified CVB3 as a useful virotherapeutic agent against NSCLC via large-scale screenings with 28 strains of human enteroviruses (Fig. 1).

Discriminatory mechanisms for selectively targeting cancer cells are a prerequisite for therapeutic oncolytic viruses. CVB3 possessed cancer-specific viral tropism, as evidenced by an extremely low infection of MOI = 0.001 (Fig. 1B). In addition, CVB3-induced cytotoxicity positively correlated with the expression levels of DAF and particularly CAR on NSCLC cells (Fig. 2). CAR is expressed on various histologic types of human lung cancers, but not on normal alveolar epithelial cells (31). DAF counteracts the cytolytic action of the complement system and whose expression is upregulated on the surface of many tumors, seems to be a good target for oncolytic virus (32). These findings form a basis for the use of CVB3 in therapeutic applications for NSCLC patients.

Our results showed a moderate contribution of caspase-mediated apoptosis to CVB3-mediated oncolysis in human NSCLC cells (Fig. 3D). Generally, a wide range of cancers are known to be resistant to apoptosis following chemotherapy (33). Thus, the ability of CVB3 to induce apoptosis is an attractive property for the treatments of refractory NSCLC (34, 35). A role of PI3K/Akt signaling in accelerating CVB3 replication in NSCLC cells was also shown by use of cotreatment with a PTEN inhibitor and CVB3 infection (Fig. 4F and G). Overexpression of p-Akt and loss of PTEN expression in NSCLC

Downloaded from cancerres.aacrjournals.org on April 19, 2015. © 2012 American Association for Cancer Research.

Published OnlineFirst March 29, 2012; DOI: 10.1158/0008-5472.CAN-11-3185

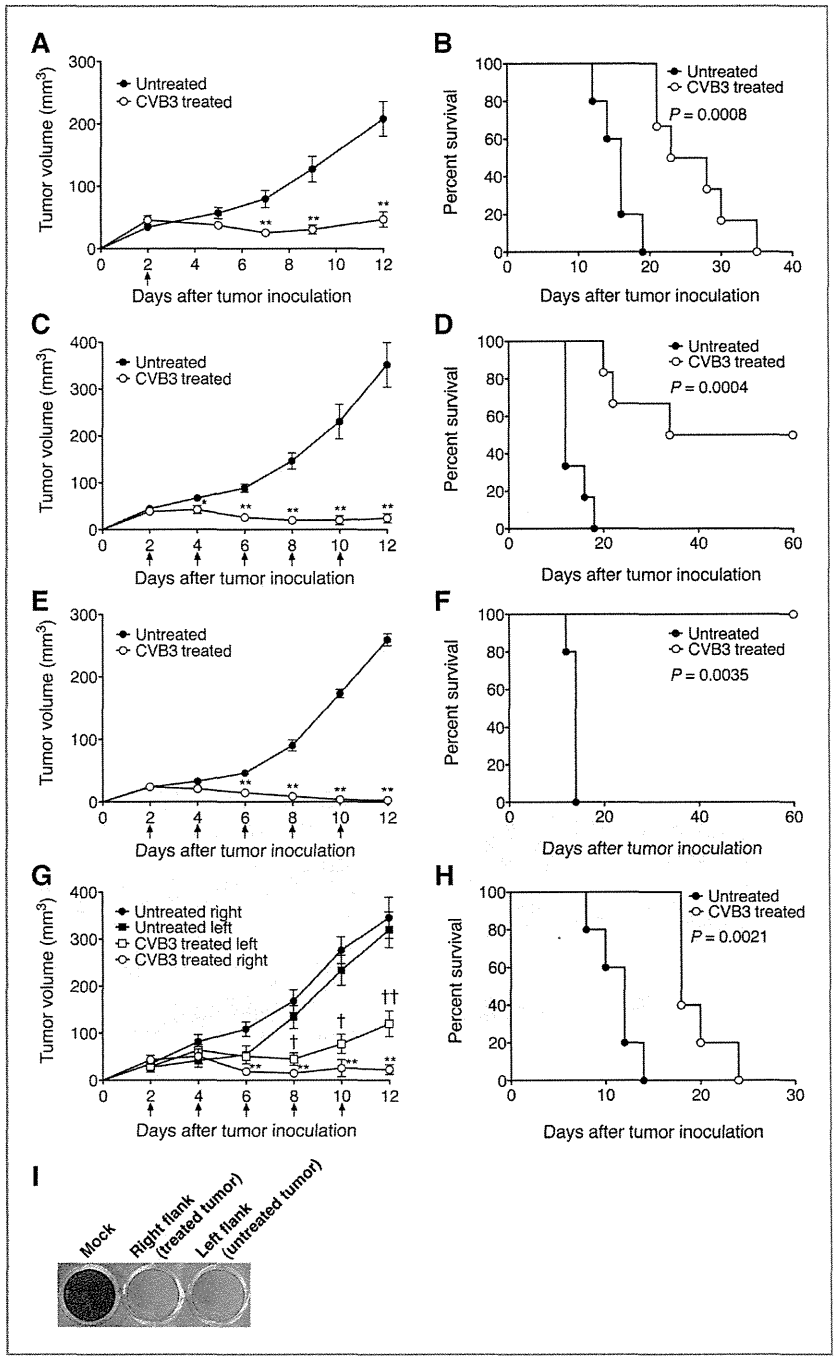

Figure 5. *In vivo* oncolytic effect of intratumoral CVB3 administration on various human NSCLC xenografts. A549 ($n = 5$ or 6; A and C) or EBC-1 ($n = 5$; E) were subcutaneously injected into the right flanks of nude mice. Each mouse received either a single dose (A), or 5 doses (C and E) of CVB3 intratumorally. Tumor volumes are expressed as means ± SEM. *, $P < 0.05$; **, $P < 0.01$. Kaplan–Meier survival analyses are shown for CVB3-treated mice with the single dose (B; $P = 0.0008$) or 5 doses (D; A549, $P = 0.0004$; F; EBC-1, $P = 0.0035$) of the CVB3. G, administration of CVB3 to the right tumor was carried out to the nude mice with bilateral tumors ($n = 5$). *, †, $P < 0.05$; **, ††, $P < 0.01$. Each symbol represents the statistical significance of right (*) and left (†) lateral tumors between untreated and CVB3-treated mice. H, Kaplan–Meier survival analyses of the mice in G are shown ($P = 0.0021$). I, two days after the CVB3 administration, the culture supernatants obtained from bilateral tumors were evaluated for oncolytic activity against cultured A549 cells.

patients was reported to confer poor differentiation, distant metastasis, and poor prognosis (36). In addition, PI3K/Akt pathway–related genes are frequently activated in diverse human cancers including NSCLC tumors (37), and cancer stem cells after systemic chemotherapy (38, 39). These findings suggest that CVB3 treatment may be suitable for NSCLC patients refractory to conventional chemotherapies. In contrast, our finding that PI3K inhibition reduced CVB3

Downloaded from cancerres.aacrjournals.org on April 19, 2015. © 2012 American Association for Cancer Research.

Published OnlineFirst March 29, 2012; DOI: 10.1158/0008-5472.CAN-11-3185

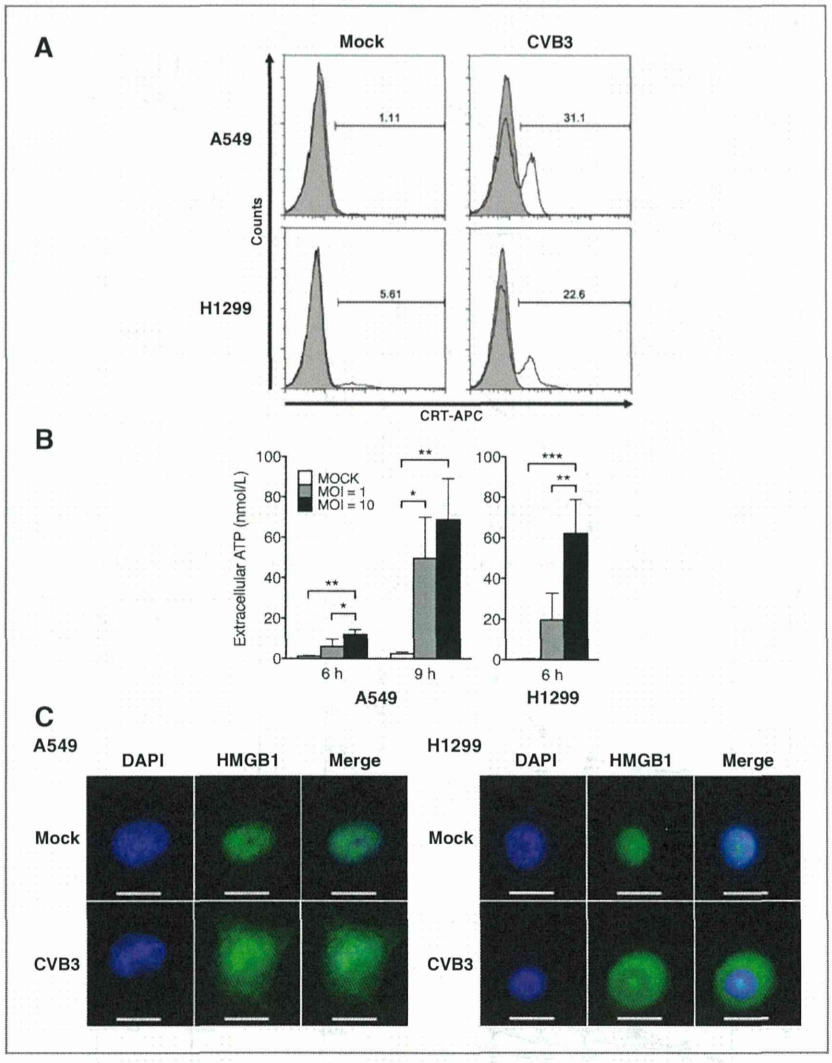

Figure 6. Induced immunogenicity in CVB3-infected NSCLC cells. A, CRT expression on the surface of A549 and H1299 cells was analyzed at 6 hours after CVB3 infection (MOI = 10) by flow cytometric analysis. B, cells were infected with CVB3 at MOI of 1.0 or 10, incubated for 6 or 9 hours, and the concentration of extracellular ATP in the culture medium was measured. Results are shown as means ± SD. *, $P < 0.05$; **, $P < 0.01$; ***, $P < 0.001$. C, immunofluorescence microscopy images of HMGB1 released from nuclei to cytosol in A549 cells infected with CVB3 for 7 hours. Cells were stained with anti-HMGB1 (green) antibody and DAPI (blue), and analyzed by fluorescence microscopy. Scale bars, 10 μm.

production from NSCLC cells raises the possibility that the use of PI3K inhibitors might regulate undesired CVB3 replication. The activity of ERK, the downstream target of MEK in the MEK/ERK survival pathway, was also closely correlated with CVB3-mediated cytotoxicity. Enhanced activation of MEK/ERK has been detected in 34% of 111 primary NSCLC patients with lower survival, but not in normal lung tissue (40, 41), providing further insight into the interplay of CVB3 replication with cellular components to improve antitumor efficacies.

It is noteworthy that intratumoral CVB3 administrations showed significant antitumor effects against A549 adenocarcinoma xenografts resistant to radiotherapy (42) and the EGFR tyrosine kinase inhibitor, gefitinib (43), EBC-1 squamous cell carcinoma (Fig. 5E and F), and H1299 adenocarcinoma xenografts (Supplementary Fig. S3), indicating that CVB3 could be a favorable therapeutic agent for patients with advanced NSCLC refractory to conventional radiotherapies and/or molecular targeted therapies.

Intratumoral CVB3 administration into one of 2 bilateral subcutaneous xenografts elicited significant suppression of growth of the distant uninjected tumors in which oncolytic CVB3 progeny could be detected. This implies that the administered CVB3 replicated, and its progeny circulated via the blood or lymphatic system and infected distant tumors, which is a beneficial for the systemic treatment of metastatic or disseminated tumors.

For toxicity evaluation, we conducted biochemical and histologic assays during CVB3 treatment. CVB3 administration induced moderate hepatic dysfunction (Supplementary Fig. S4A), with no histologic evidence of active hepatitis

Downloaded from cancerres.aacrjournals.org on April 19, 2015. © 2012 American Association for Cancer Research.